Over-expression of Rififylin, a new RING finger and FYVE-like domain-containing protein, inhibits recycling from the endocytic recycling compartment.

Franck Coumailleau, Vincent Das, Andres Alcover, Graça Raposo, Sandrine Vandormael-Pournin, Stéphanie Le Bras, Patricia Baldacci, Alice Dautry-Varsat, Charles Babinet, Michel Cohen-Tannoudji

Molecular Biology of the Cell
Vol. 15, 4444–4456, October 2004

Over-Expression of Rififylin, a New RING Finger and FYVE-like Domain-containing Protein, Inhibits Recycling from the Endocytic Recycling Compartment

Franck Coumailleau,* Vincent Das,† Andres Alcover,† Graça Raposo,‡ Sandrine Vandormael-Pournin,* Stéphanie Le Bras,*§ Patricia Baldacci,*‖ Alice Dautry-Varsat,† Charles Babinet,* and Michel Cohen-Tannoudji*¶

*Unité Biologie du Développement, CNRS URA 2578, Institut Pasteur, 75724 Paris Cedex 15, France; ‡Electron Microscopy of Intracellular Compartments, CNRS UMR 144, Institut Curie, 75248 Paris Cedex 05, France; and †Unité de Biologie des Interactions Cellulaires, Centré National de la Recherche Scientifique URA 2582, Institut Pasteur, 75724 Paris Cedex 15, France

Submitted March 31, 2004; Accepted June 4, 2004
Monitoring Editor: Keith Mostov

Endocytosed membrane components are recycled to the cell surface either directly from early/sorting endosomes or after going through the endocytic recycling compartment (ERC). Studying recycling mechanisms is difficult, in part due to the fact that specific tools to inhibit this process are scarce. In this study, we have characterized a novel widely expressed protein, named Rififylin (Rffl) for RING Finger and FYVE-like domain-containing protein, that, when overexpressed in HeLa cells, induced the condensation of transferrin receptor-, Rab5-, and Rab11-positive recycling tubulovesicular membranes in the perinuclear region. Internalized transferrin was able to access these condensed endosomes but its exit from this compartment was delayed. Using deletion mutants, we show that the carboxy-terminal RING finger of Rffl is dispensable for its action. In contrast, the amino-terminal domain of Rffl, which shows similarities with the phosphatidyl-inositol-3-phosphate–binding FYVE finger, is critical for the recruitment of Rffl to recycling endocytic membranes and for the inhibition of recycling, albeit in a manner that is independent of PtdIns(3)-kinase activity. Rffl overexpression represents a novel means to inhibit recycling that will help to understand the mechanisms involved in recycling from the ERC to the plasma membrane.

INTRODUCTION

Endocytosis is a fundamental cellular process, whereby extracellular material as well as plasma membrane proteins and lipids are internalized and transported to various intracellular compartments (Mukherjee *et al.*, 1997). Initially, internalized molecules are delivered to early/sorting endosomes, which constitute the first sorting station of the pathway. Ligands may dissociate from their receptor at the mildly acidic pH of the early/sorting endosomes and are then targeted to the late endosome degradation compartment, whereas receptors may be transported back to the plasma membrane through recycling endosomes. Underlying the complexity and dynamic nature of the endocytic compartment, a large array of cellular proteins act together to ensure complex sorting decisions and precise targeting of internalized molecules.

About 95% of endocytosed membrane is recycled to the plasma membrane. This recycling is important for the maintenance of membrane composition and for receptors involved in nutrient uptake as well as for other several cellular processes. To study the recycling pathway, the transferrin receptor (TfR) and its ligand transferrin (Tf) have been used extensively (reviewed in Mellman, 1996; Mukherjee *et al.*, 1997; Maxfield and McGraw, 2004). Within early endosomes, Fe^{3+} dissociates from Tf and the TfR-Tf complexes, either return directly to the plasma membrane or reach a network of tubular membranes, called the endocytic recycling compartment (ERC) before returning to the plasma membrane. These two pathways are believed to rely on distinct molecular machineries and the functional significance of these two recycling pathways is poorly understood. Some evidence indicates that ERC has sorting abilities. Indeed, ERC has been shown to be instrumental in basolateral/apical sorting in epithelial cells (Apodaca *et al.*, 1994; Knight *et al.*, 1995) as well as to be involved in the delivery of membrane proteins to the *trans*-Golgi network (TGN; Ghosh *et al.*, 1998). ERC may therefore represent, in addition to early/sorting endosomes, another sorting station along the recycling pathway.

Only a few molecules involved in the function of the ERC have been identified so far. Among the large Rab family (Zerial and McBride, 2001), Rab11 has been shown to local-

Article published online ahead of print. Mol. Biol. Cell 10.1091/mbc.E04–04–0274. Article and publication date are available at www.molbiolcell.org/cgi/doi/10.1091/mbc.E04–04–0274.

Present addresses: § Department of Biology, The Johns Hopkins University, Baltimore, MD 21218; ‖ Biologie et Génétique du Paludisme, Département de Parasitologie, Institut Pasteur, Paris Cedex 15, France.

¶ Corresponding author. E-mail address: m-cohen@pasteur.fr.

Abbreviations used: DAPI, 4′,6-diamidino-2-phenylindole; ERC, endocytic recycling compartment; MVB, multivesicular bodies; PAG, protein A gold conjugate; PtdIns(3)P, phosphatidyl-inositol-3-phosphate; RACE, rapid amplification of cDNA ends; Rffl, Rififylin; Tf, transferrin; TfR, transferrin receptor; TGN, *trans*-Golgi network.

ize to and to function in endocytic recycling from the ERC to the plasma membrane (Ullrich *et al.*, 1996) and the TGN (Wilcke *et al.*, 2000). Several Rab11-interacting proteins have been isolated: Rab11BP/Rabphillin11 (Zeng *et al.*, 1999), myosin Vb (Lapierre *et al.*, 2001), and members of the Rab11-FIP family (Lindsay *et al.*, 2002; Lindsay and McCaffrey, 2002; Meyers and Prekeris, 2002; Wallace *et al.*, 2002a, 2002b). Overexpression of truncated versions of some of these proteins alters the morphology of the Rab11-positive compartment, sometimes affecting Tf recycling, indicating that they participate in the functions of Rab11 in the ERC. Syntaxin13, a member of the SNARE protein family, is found preferentially associated with recycling endosomes, where it plays a role in membrane fusion events during recycling of plasma membrane proteins (Prekeris *et al.*, 1998). Rme-1, a protein identified in a genetic screen for endocytosis mutants in *Caenorhabditis elegans*, has been reported to be involved in the exit of membrane proteins from the ERC to the TGN and the plasma membrane (Lin *et al.*, 2001). Altogether, very little is known about the regulation of membrane trafficking through the ERC (Maxfield and McGraw, 2004). A major difficulty stems from the paucity of specific tools to inhibit recycling and from the existence of several recycling pathways.

We have identified a novel gene coding for a protein, Rififylin (Rffl), containing both a FYVE-like domain and a RING finger in the amino- and carboxy-terminal region, respectively. Using deletion mutant analysis, we found that the amino-terminal domain is a key component of Rffl. This domain presents sequence similarities with the well-characterized phosphatidyl-inositol-3-phosphate (PtdIns(3)P)-binding FYVE finger. It is instrumental for Rffl recruitment to recycling endosome, but in contrast to FYVE fingers, is not dependent on PtdIns(3)-kinase activity. We show that overexpression of Rffl alters both the morphology and the function of recycling endosomes, as illustrated by the massive accumulation of TfR and Rab11 in the perinuclear region and the inhibition of Tf recycling.

MATERIALS AND METHODS

Plasmid Constructs

cDNA sequences encoding the full-length 363 amino acid coding region of Rffl were PCR-amplified from mouse liver mRNA using the primer 5′F5 (5′-GTTCTCGAGCCACCATGTGGGCATCCTGCTGCAACT) that contains an *Xho*I site and a Kozak translational start consensus, and the primer 3′F2 (5′-ACCGGTGGATCCGGGGACCGGAAGACGTGCACTGCT), which includes a *Bam*HI sequence. The resulting sequence was cloned into the *Xho*I and *Bam*HI sites of pEGFP-N1 (Clontech, Palo Alto, CA) to give rise to a mouse-Rffl-GFP expression vector. We also derived an expression vector for the Rffl protein fused in its amino-terminal region with GFP (GFP-Rffl). This was achieved by subcloning the full-length coding region of Rffl from Rffl-GFP into the *Bgl*II and *Bam*HI sites of pEGFP-C1 (Clontech). The myc-Rffl expressing vector was obtained by PCR amplification on mouse liver cDNA by using the primers 5′m3c (5′-CGAGATCTTCATGTGGGCATCCTGCTGCAACTGGT) and 3′m3c (5′-CGGAATTCTCAGGACCGGAAGACGTGCACT) and cloned into the *Bam*HI and *Hin*dIII sites of pCMV-Tag3c (Stratagene, La Jolla, CA). Untagged Rffl-expressing vector was obtained after deletion of GFP in the Rffl-GFP construct. Two mutants that lack either residues 3/98 from the N-terminus (Rffl-GFP-ΔNter) or residues 336/363 from the C-terminus (Rffl-GFP-ΔCter) were generated by restriction enzymes digestion. Rffl-GFP-ΔNter was obtained after digestion of Rffl-GFP construct with *Xho*I/*Sac*I and religation with annealed oligonucleotides 5′D0 (TCGACCACCATGTGGGAGGAGCT) and 3′D0 (CCTCCCACATGGTGG). Rffl-GFP-ΔCter was obtained after digestion of Rffl-GFP construct with *Bst*EII/*Bam*HI and religation with annealed oligonucleotides 5′D3 (GTGACTCCT) and 3′D3 (GATCAGGA). The single-FYVE (SFL) and double-FYVE (DFL) constructs consist of one and two copies of residues 4–95 fused to pEGFP-N1 (Clontech). Junctions and PCR-amplified regions were sequenced to ensure that no errors were introduced.

Cell Culture and Transient Transfections

HeLa cells were grown at 37°C in the presence of 8% CO_2 in DMEM supplemented with 10% FCS (complete medium) and transiently transfected by electroporation as follows: cells (6×10^6/200 μl of complete medium) were placed in 0.45-cm gap cuvette along with 10–30 μg of plasmid DNA and electroporated (200 V and 975 μF) with a Bio-Rad GenePulser II (Richmond, CA). Under these conditions, we observed that 70–90% of transfected cells expressed Rffl-GFP. Cells were then plated on 12-mm gelatin-coated glass coverslips and processed for immunofluorescence analysis 4 or 16 h after electroporation. Treatment with wortmannin (Sigma, St. louis, MO) was carried out at 100 nM for 40 min at 37°C. Concentration of the drug and duration of the treatment were increased up to 400 nM and 3 h, respectively. Treatment with LY294002 (Calbiochem, San Diego, CA) was carried out at 100 μM for 40 min at 37°C.

Immunofluorescence Microscopy

Transfected cells were washed in PBS, fixed for 20 min in 4% PFA, and incubated twice for 8 min in PBS-glycine, 0.1 M, before immunostaining. The cells were then blocked in PSBS buffer (PBS supplemented with 10% FCS, 0.2% BSA, and 0.05% of saponin) for 20 min at room temperature. Primary and secondary antibody incubations were performed in PSBS buffer for 1 h at room temperature. Monoclonal antibodies against EEA1, GM130, and Rab5 were from Transduction Laboratories (Lexington, KY). Monoclonal anti-TfR and anti-myc antibodies were from Sigma. Monoclonal anti-Lamp2 was from Pharmingen (San Diego, CA). Rabbit polyclonal anti-Rab11 and anti-Rab6 were a generous gift from Jean Salamero and Bruno Goud (Institut Curie, Paris). Rabbit polyclonal anti-TGN38 was obtained from George Banting. Alexa^{498}- and Alexa^{594}-conjugated secondary antibodies were from Molecular Probes (Eugene, OR). Coverslips were mounted in mowiol containing 100 mg/ml DABCO (Sigma) and examined using a Zeiss LSM 510 confocal microscope (Thornwood, NY). *Z*-series of optical sections were acquired at 0.3-μm increments. Images were acquired with a setting allowing the maximum detection below saturation limits. For double staining, sequential acquisitions per optical section were performed, in order to prevent fluorescence passage between the two channels. Three-dimensional reconstructions using 36 projections around the *Y* axis were performed using LSM-510 software. Images were processed using Adobe Photoshop v5.0 software (San Jose, CA). Other images were obtained using a Zeiss Axioplan 2 fluorescence microscope equipped with a Zeiss AxioCam camera.

Immunoblotting

Recombinant fusion protein of the FYVE-like domain of Rififylin (1–100 amino acids) was produced in *Escherichia coli* as a GST fusion protein from pGEX-4T1 expression vector (Pharmacia Biotechnology, Piscataway, NJ) and purified using a gluthathione-conjugated affinity column (Pharmacia Biotech). Purified protein (37 kDa) was then used as an immunogen for the production of rabbit antiserum (Agro-Bio, La Ferté Saint-Aubin, France). Serum batches showing higher titers were subjected to antigen-affinity chromatography. Although the antigen-affinity purified anti-Rffl antibody allowed the detection of overexpressed Rffl, they never detected endogenous Rffl. In addition, it cross-reacted with many unidentified proteins (see Figure 5B, right panel). For immunoblotting, total cell lysates were subjected to SDS-polyacrylamide gel elecrophoresis and transferred to nitrocellulose by standard methods. The blots were then probed with affinity-purifified anti-Rffl (1/1000 dilution) or anti-GFP (Clontech, 1/7500 dilution) and peroxidase-conjugated anti-rabbit antibodies (Jackson ImmunoResearch Laboratories, West Grove, PA, 1/50 000 dilution) followed by ECL detection (Pharmacia Biotechnology).

Transferrin Recycling Assays

Tf recycling was first monitored using a fluorescence microscope. Sixteen hours after transfection, HeLa cells were incubated for 90 min in a serum-free medium supplemented with 0.1% BSA. Then, cells were allowed to internalize Alexa^{594}-Tf (Molecular Probes) for 90 min at 37°C and washed three times in ice-cold PBS. Recycling was induced by warming up the cells to 37°C in medium containing 0.1% BSA and a 100-fold excess of unlabeled holotransferrin (Sigma). At various times, cells were washed three times in ice-cold PBS, fixed, stained with DAPI, and observed under a fluorescence microscope. Quantification of Tf recycling was performed by flow cytometry. Cells were transfected with plasmids encoding Rffl-GFP or GFP. Sixteen hours later, transfected cells were incubated for 30 min in a serum-free medium at 37°C, and Alexa^{633}-Tf (Molecular Probes) was added for 30 min at 37°C. The cells were then washed in serum-containing medium at 4°C, and membrane-bound Tf was removed by acid wash (DMEM medium, 20 mM sodium acetate, pH 3.0, for 3 min at 4°C), followed by neutralization with an excess of DMEM medium, 30 mM HEPES buffer, pH 7.4, as described in Duprez *et al.* (1988). The efficiency of acid wash of cell surface Tf was more than 97%. Recycling was then induced by rapidly warming up the cells to 37°C, in DMEM medium containing a 100-fold excess of unlabelled Tf. When indicated, 100 μM LY294002 was added to loading and recycling medium. At various times, recycling was stopped by adding ice-cold DMEM medium

supplemented with 10% fetal calf serum. Fluorescence intensity due to GFP and to Alexa^{633}-Tf was then measured by flow cytometry (FACS-LSR, BD Biosciences, San Diego, CA). The mean fluorescence intensity of 10,000 cells expressing Rffl-GFP or GFP was obtained for each time point.

Electron Microscopy

Transfected HeLa cells were fixed with a mixture of 2% PFA and 0.2% glutaraldehyde in 0.2 M phosphate buffer, pH 7.4, for 2 h at room temperature. Cells were embedded in 10% gelatin, infused in 2.3 M sucrose, and frozen in liquid nitrogen as described previously (Raposo *et al.*, 1997). Ultrathin cryosections were prepared with a Leica FCS ultracryomicrotome (Leica, Deerfield, IL) and retrieved with a mixture of 2% methylcellulose, 2.3 M sucrose (vol/vol; Liou *et al.*, 1996). Sections were single immunogold labeled with a rabbit polyclonal anti-GFP (Molecular Probes) or double immunogold labeled using, in a first step, a mouse monoclonal anti-TfR (clone H68.4, Zymed Laboratories, South San Francisco, CA) or a mouse monoclonal anti-CD63 (clone CBL/gran, Caltag Laboratories, Burlingame, CA) followed by a rabbit anti-mouse IgG (Dako, Carpinteria, CA) and, in a second step the anti-GFP antibody. Antibodies were detected with protein A gold conjugates 10 or 15 nm (PAG 10; PAG 15) that were purchased from Department of Cell Biology, Utrecht University, The Netherlands. Double labelings were performed according to Slot *et al.* (1991). A 1% glutaraldehyde fixation step was included between the primary and the secondary antibody/protein A gold conjugates incubation steps in order to avoid the first antibody to be recognized by the second protein A gold conjugate. Controls were performed without the primary or secondary antibody reagents (Raposo *et al.*, 1997).

Northern Blot Analysis

A mouse multiple tissue Northern Blot from Clontech was hybridized in Hybridexpress buffer (Clontech) with a ^{32}P-labeled probe corresponding to *Rififylin* ORF. Hybridization and washes were performed at 68 and 50°C, respectively. Autoradiography was performed using X-Omat film (Eastman Kodak, Rochester NY).

RESULTS

Cloning of a Novel Protein that Contains Two Zinc Finger Domains

During our global effort of gene identification and characterization in the *Ovum mutant* locus region on mouse chromosome 11 (Babinet *et al.*, 1990; Cohen-Tannoudji *et al.*, 1996, 2000; Le Bras *et al.*, 2002), we have identified several ESTs that mapped in the nonrecombinant *Om* region. One of these ESTs (accession no. AA174545) from CD-1 mouse testis library was obtained from the IMAGE consortium and fully sequenced. To complete this analysis, we performed a 5′-RACE RT-PCR reaction on BALB/c testis cDNAs that yielded an additional 491-base pair 5′ cDNA fragment. The sequence of the reconstituted testis cDNA is depicted in Figure 1A. It is identical to three full-length mouse testis cDNAs that were submitted to the public databases while this work was in progress (acc no. AK007189, NM026097, and AK006757), further suggesting that our sequence corresponds to a full-length testis cDNA. This cDNA contains an ORF of 1011 nt in length that encodes a protein of 336 amino acids. Computer-based structural analysis of the ORF predicted that the protein contained one putative zinc finger domain at both the carboxy- and amino-terminal regions (Figure 1B). In the carboxy-terminal region (aa 288–322) a consensus sequence for a C_3HC_4 RING finger domain was found: $CX_2CX_{(9-39)}CX_{(1-3)}HX_{(2-3)}CX_2CX_{(4-48)}CX_2C$, where X can be any amino acid. Present in a large number of proteins, this domain has been proposed to mediate protein-protein interactions (Saurin *et al.*, 1996), and more recently, to participate in the ubiquitination process (Freemont, 2000; Weissman, 2001).

Sequence comparison indicated that the RING finger of this protein shows highest identities (45–57%) with that of inhibitors of apoptosis proteins. At the amino-terminal region, amino acids 8–93 constitute a domain related to the well-characterized FYVE domain, a double zinc finger domain that mediates specific binding to PtdIns(3)P (Stenmark *et al.*, 2002). Using the BLASTP program, we established that this region has 38% of identities and 49% of similarities with the FYVE domain of human early endosome autoantigen 1 (EEA1, aa residues 1348–1409). Interestingly, the group of basic residues, R(R/K)HHCR, which is the principal site of interaction with PtdIns(3)P is not conserved, His^3, His^4, and Arg^6 being replaced by nonbasic residues (Gln, Thr, and Leu, respectively; arrowheads on Figure 1C). Similarly, a highly conserved Gly residue located immediately after the second zinc coordinating motif is replaced by a Lys residue in this variant FYVE domain. However, conservation of zinc chelating and domain-stabilizing hydrophobic residues in this variant domain suggests that it may adopt a conformation similar to that of bona fide FYVE domain. Nevertheless, it is likely that it presents different properties, in particular regarding binding specificity. On the basis of these observations, we decided to name this gene *Rififylin* for RING Finger and FYVE-like domain-containing protein.

Analysis of tissue expression of *Rffl* showed that it was expressed in all tissues and cell lines tested. Northern blot analysis revealed a ubiquitously expressed RNA species of ~4 kb (Figure 1D). A smaller transcript of ~2 kb was detected in the testis at a very high level and in the liver at a moderate level (Figure 1D). It is likely that the testis cDNA we cloned corresponds to this small transcript. Interestingly, using RT-PCR, we identified an alternatively spliced exon of 84 nt long that adds 28 aa in the middle region of the protein (shadowed sequences on Figure 1A). In all tissues, *Rffl* transcripts harboring this 84 nt long additional sequence were detected (Figure 1E). In testis, *Rffl* transcript devoid of the additional sequence was most abundant, whereas in liver, kidney, and HeLa cells majority of *Rffl* transcripts contained the additional sequence (Figure 1E). These data suggest that *Rffl* codes for two ubiquitously expressed proteins of 336 and 364 aa, respectively, and that their relative level of expression varies between tissues. Hela cells express almost exclusively the 363 aa isoform, as do adult mouse liver and kidney cells.

Overexpression of Rififylin Affects the Morphology of Recycling Endosomes

We first examined the intracellular distribution of Rffl in HeLa cells. We constructed a vector expressing the full-length (363 aa) protein fused, at its C-terminus, to GFP (Rffl-GFP). HeLa cells were electroporated with this vector and the distribution of the fusion protein was examined 16 h later. In most cells, we observed that Rffl-GFP localized to a limited number of brightly stained globular structures at the perinuclear region (Figure 2, left panels). This situation was not restricted to HeLa cells because similar globular structures were observed upon expression of Rffl-GFP in various cell types (COS7, mouse embryonic fibroblasts, Neuro2A, AtT20p, MDCK, or LLCPK; our unpublished results). Moreover, this phenotype was due to Rffl overexpression per se because similar observations were made in cells expressing either untagged Rffl (detected using anti-Rffl antibody), the Rffl protein tagged with GFP in its N-terminus (GFP-Rffl), or with a c-myc epitope at the N-terminus (myc-Rffl; our unpublished results).

We analyzed the structures labeled by Rffl-GFP in transfected cells, with markers from subcellular compartments. In cells overexpressing Rffl, the pattern of some endosomal markers was perturbed. Thus, TfR, a marker of peripheral early endosomes and perinuclear recycling endosomes, was severely redistributed in Rffl-GFP expressing cells as most TfR immunostaining was detected in aggregated perinuclear structures in these cells. Although we observed that TfR and

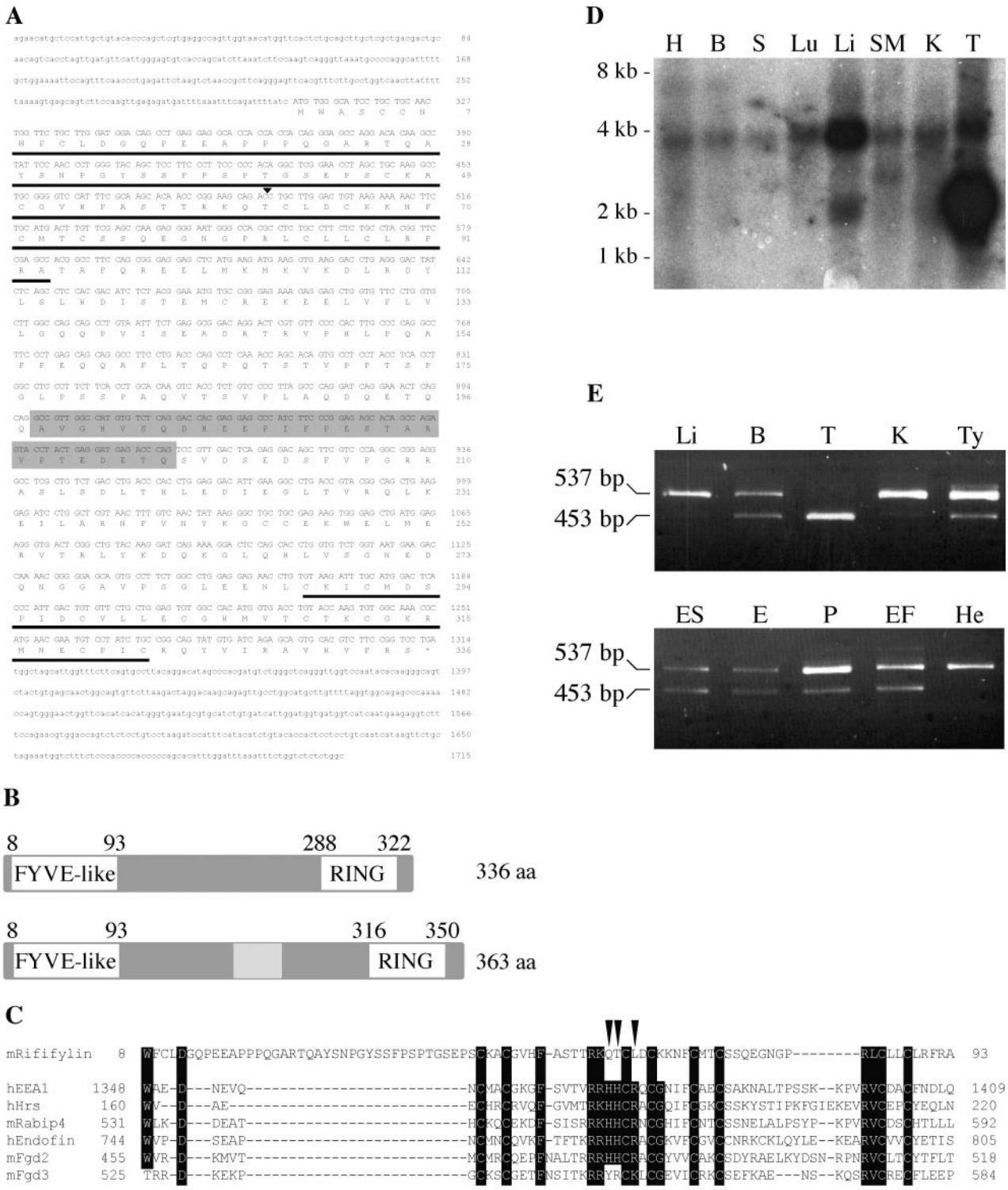

Figure 1. *Rifiylin* expression and protein structure. (A) Nucleotide and predicted amino acid sequence of mouse *Rffl* cDNA. Sequences 5′ of nt 492 (arrowhead) have been derived from a testis 5′RACE RT-PCR product. The FYVE-like and RING domains are underlined. The alternative coding sequence is shadowed and not numbered. Sequence data for the testis cDNA and the alternative coding sequence are available from GenBank/EMBL/DDBJ under accession nos. AY163902 and AY163903, respectively. (B) Schematic representation of the two Rffl protein isoforms. (C) ClustalW alignments of Rffl FYVE-like domain with previously characterized FYVE domains. The amino-acids that defined the FYVE finger signature (Stenmark *et al.*, 2002) are indicated in bold. Arrowheads point to critical residues of the core R(R/K)HHCR motif that are not conserved in the FYVE-like domain. (D) Northern blot (mouse MTN, Clontech) and (E) RT-PCR analysis of *Rffl* expression in adult mouse and embryonic tissues: heart (H), brain (B), spleen (S), lung (Lu), liver (Li), skeletal muscle (SM), kidney (K), testis (T), thymus (Ty), embryo 14.5 dpc (E), placenta 14.5 dpc (P), and in ES cells (ES), mouse embryonic fibroblasts (EF), and human HeLa cells (He). Region from nt 662-1115 was amplified by RT-PCR. PCR products of 537 and 453 base pairs in length correspond to transcripts with and without the alternative coding sequence, respectively.

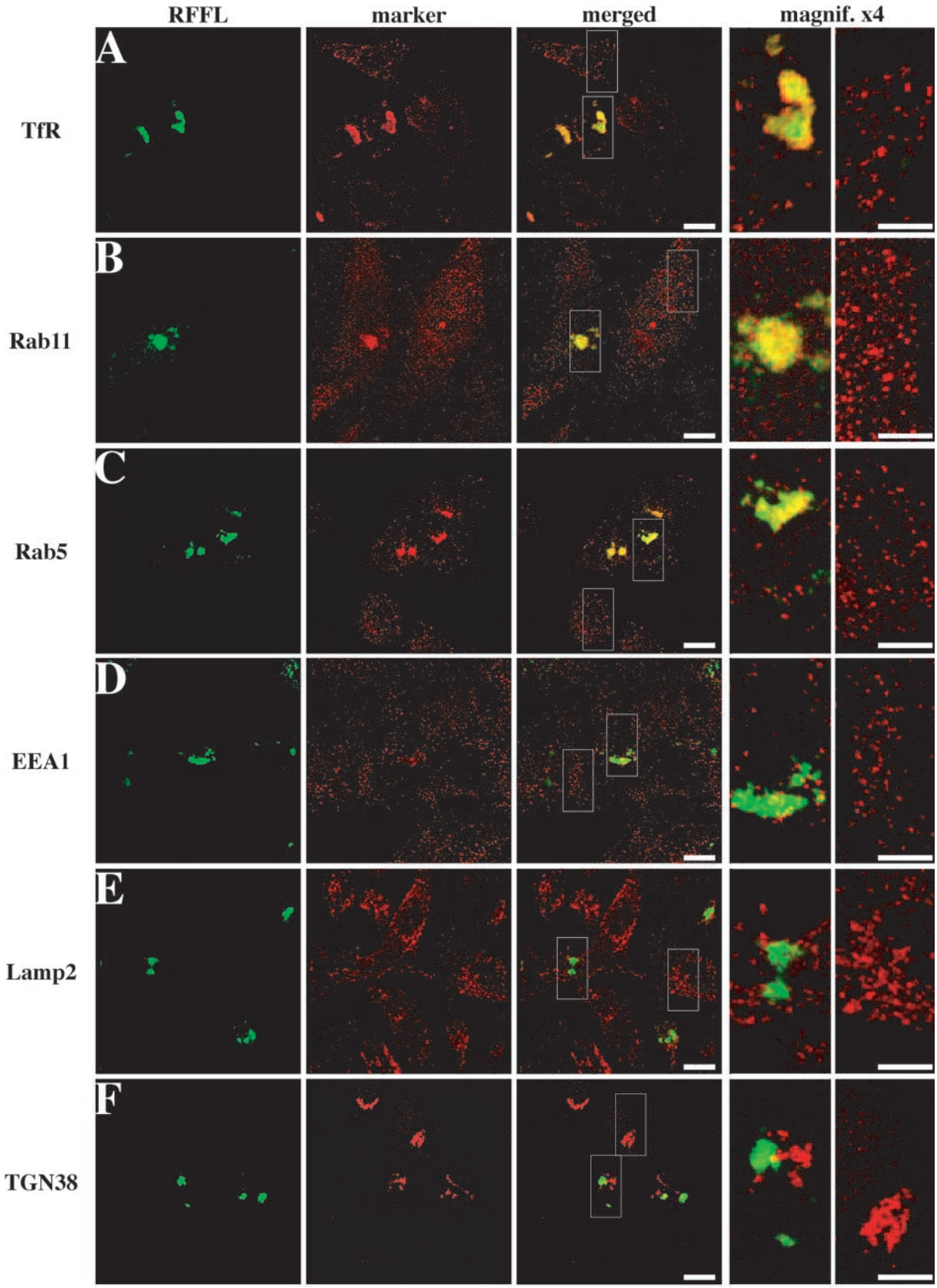

Figure 2. Effects of Rififylin overexpression on the morphology of endocytic compartments. HeLa cells were transfected with Rffl-GFP expressing vector and analyzed 16 h post-transfection. Transfected cells were fixed, immunostained with antibodies against TfR (A), Rab11 (B), Rab5 (C), EEA1 (D), Lamp2 (E), and TGN38 (F), and analyzed by confocal microscopy. Images show a medial orientation of a three-dimensional reconstruction. Bars, 10 μm. In each case, the right panel shows a higher magnification of the area delimited by the insets showing the Rffl-positive compartment (magnification, $\times$4, left) and the corresponding area of a nontransfected cell (magnification, $\times$4, right). Bars, 5 μm.

Rffl-GFP colocalized to some extent, the two markers often appeared tightly intermingled but not fully colocalized (Figure 2A). Similarly, immunostaining of Rab11, a marker of the ERC and TGN, or Rab5, a marker of early endosomes, were shifted to the Rffl-positive structures (Figure 2, B and C). In contrast, the staining of EEA1, a marker of early/sorting endosomes, was unaffected by Rffl overexpression and appeared as a punctate vesicular pattern indistinguishable from that observed in untransfected HeLa cells (Figure 2D). Finally, we found that Rffl-positive structures were distinct from Lamp2-positive late endosomes/lysosomes (Figure 2E) and from the *trans*-Golgi network, labeled with an anti-TGN38 antibody (Figure 2F). Moreover, other Golgi markers, such as GM130 and Rab6, were unaffected by Rffl overexpression (our unpublished results). It is intriguing that Rab5 and EEA1 localization were differentially affected by Rffl overexpression. Indeed, it was reported that Rab5 physically interacts with EEA1 and colocalizes with it in early endosomes, where it regulates the homotypic fusion between early endosomes as well as the transport of clathrin-coated vesicles from the plasma membrane to early endosomes (Gorvel *et al.*, 1991; Bucci *et al.*, 1992; Stenmark *et al.*, 1994). Altogether, these data suggest that Rffl-positive structures belong to the endocytic recycling compartment. It should also be noted that the condensation of endosomal structures upon Rffl overexpression did not appeared to be due to the disorganization of cytoskeleton networks because similar distributions of actin and tubulin were observed in Rffl-transfected and nontransfected cells (our unpublished results).

To gain further insight as to the nature of the endosomal membranes in which Rffl-GFP accumulates, we analyzed the subcellular distribution of Rffl on ultrathin cryosections of transfected HeLa cells. We observed that the Rffl-positive compartment consisted of massive accumulation of tubulovesicular membrane profiles decorated with Rffl at high density (Figure 3A). In addition, we observed some Rffl staining on the outer membranes of vacuolar structures containing a few internal membranes (star on Figure 3A). In agreement with our immunofluorescence data, double immunogold labeling revealed an intermingled distribution of Rffl (10-nm gold particles) and TfR (15-nm gold particles) in the tubulovesicular membrane profiles (Figure 3B). In contrast, double immunogold labeling of Rffl and CD63, a protein present in late endosomes and lysosomes of HeLa cells (Stumptner-Cuvelette *et al.*, 2003), indicated that the two proteins localized to distinct membranes subdomains, CD63 being mostly restricted to the internal membranes of endosomal compartments (star on Figure 3C). In conclusion, morphological analysis revealed that aggregation of perinuclear TfR positive tubules is the main phenotype induced by Rffl overexpression.

Overexpression of Rififylin Slows Tf Recycling from the ERC

The morphological alteration of the endosomal compartment induced by Rffl expression prompted us to investigate whether Rffl overexpression could alter protein traffic in this compartment. To follow the recycling of Tf from the ERC to the cell surface, transfected cells were first allowed to internalize Alexa^{594}-Tf at 37°C for 90 min and then were subjected to a chase with an excess of unlabeled Tf for various times. Initially, Alexa^{594}-Tf was found in vesicular structures in the perinuclear area of the cytoplasm as well as in the cell periphery of the nontransfected cells (Figure 4A). In Rffl-overexpressing cells, Alexa^{594}-Tf was found accumulated in the perinuclear Rffl-positive structures (Figure 4A). Some Tf-containing vesicles were also present in the peripheral cytoplasm but to a lesser extent than in nontransfected cells (Figure 4A). After 30 min, most labeled Tf was chased from nontransfected cells (Figure 4B). In contrast, in Rffl-expressing cells, Alexa^{594}-Tf had disappeared from peripheral vesicles, but a significant amount was retained in the Rffl-positive compartment up to a 240-min chase (Figure 4, B–D).

Quantification of the effect of Rffl-GFP expression on the kinetics of Tf recycling was performed by flow cytometry. Rffl-GFP– and GFP-transfected cells were loaded for 30 min at 37°C with Alexa^{633}-Tf. Then, plasma membrane-associated Alexa^{633}-Tf was removed by an acid wash at 0°C, and the cells were incubated at 37°C to allow recycling of internalized Tf. Fluorescence intensity due to Alexa^{633}-Tf in cells transfected with Rffl-GFP was then compared with that of control cells transfected with GFP. The rate of Alexa^{633}-Tf recycling was significantly lower in Rffl-expressing cells than in control cells (Figure 4E). Consistently, the surface levels of TfR were reduced by twofold in Rffl-GFP–positive cells as compared with controls (our unpublished results). Altogether, these data show that overexpression of Rffl significantly slows recycling from the ERC to the plasma membrane.

The Amino-terminal FYVE-like Domain Is Essential for the Effect of Rififylin on Recycling Endosomes

To study the role of Rffl zinc finger domains, we constructed expression vectors coding for deletion mutants of Rffl lacking either the amino-terminal FYVE-like domain or the carboxy-terminal RING finger motif (Figure 5A). GFP-tagged full-length and truncated Rffl proteins were expressed in HeLa cells (Figure 5B). Rffl-ΔCter harbors a truncated and therefore nonfunctional RING finger. Its distribution was undistinguishable from that of full-length Rffl (Figure 5, D and C, respectively). In contrast, Rffl-ΔNter was uniformly distributed in the cytoplasm and the nucleus (Figure 5E). This pattern was indistinguishable from that of GFP alone (our unpublished results). We next analyzed the effect of overexpression of the deleted proteins on Tf recycling. The kinetics of Tf recycling was not affected by the expression of Rffl-ΔNter, whereas Rffl-ΔCter induced an inhibition of Tf recycling similar to that of full-length Rffl (Figure 5F).

Because the intracellular localization of Rffl required the presence of the FYVE-like domain, we constructed expression vectors coding for one (SFL), or two tandemly arranged (DFL), Rffl FYVE-like domain fused to GFP. When expressed in HeLa cells, SFL-GFP was mainly cytosolic, whereas DFL-GFP localized on vesicular structures (Figure 6, A and B). Immunofluorescence analysis showed that DFL-GFP and TfR partially colocalized (Figure 6C). Morphological alteration of the endocytic compartment was less pronounced upon expression of DFL-GFP than Rffl-GFP. Thus, vesicular structures containing DFL-GFP were smaller and more dispersed in the cytoplasm than those containing full-length Rffl-GFP (compare Figures 2 and 6C). Yet, inhibition of Tf recycling was similar in DFL-GFP– and Rffl-GFP–expressing cells (Figure 6D). Altogether, these results indicate that the Rffl amino-terminal FYVE-like domain is necessary and sufficient for targeting Rffl to the ERC and to inhibit Tf recycling. In contrast, the carboxy-terminal zinc finger domain is dispensable for the effect mediated by Rffl overexpression on recycling endosomes.

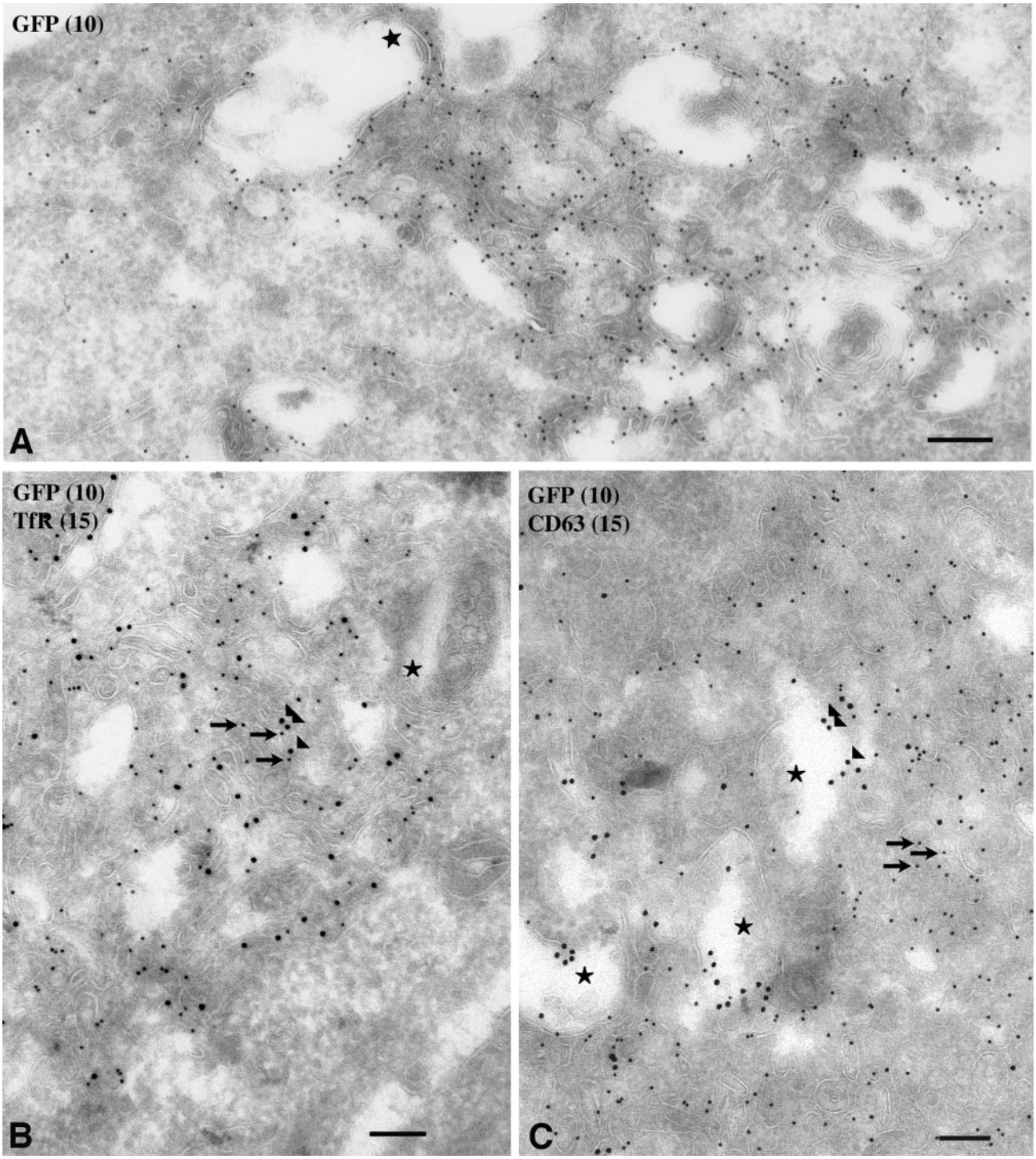

Figure 3. Localization of Rifyfilin-GFP by electron microscopy. Ultrathin cryosections of transfected HeLa cells were single immunogold labeled with anti-GFP and protein A Gold conjugate (PAG10, 10 nm) (A) and double immunogold labeled for TfR (PAG15, 15 nm) and GFP (PAG10) (B) or for CD63 (PAG15) and GFP (PAG10) (C). Cells overexpressing Rffl-GFP display a tubulo-vesicular network of membranes in close apposition to vacuolar endosomes. Rffl-GFP accumulates in these tubulo-vesicular membranes (A). The TfR accumulates in tubulo-vesicular structures together with Rffl-GFP (B). CD63 is detected in late endosomes/lysosomes that are often close to the Rffl-positive tubules (C). Arrows: 10-nm gold particles; arrowheads: 15-nm gold particles; stars: late endosomes/lysosomes. Bars, 200 nm.

The effect of Rififylin Is Independent of PtdIns(3)-kinase Activity

The amino-terminal zing finger domain of Rffl resembles the FYVE domain that has been shown to bind specifically to PtdIns(3)P (Burd and Emr, 1998; Gaullier *et al.*, 1998; Patki *et al.*, 1998). However, it exhibits important sequence differences (see above), suggesting that Rffl might not bind to PtdIns(3)P. To investigate this point, HeLa cells expressing

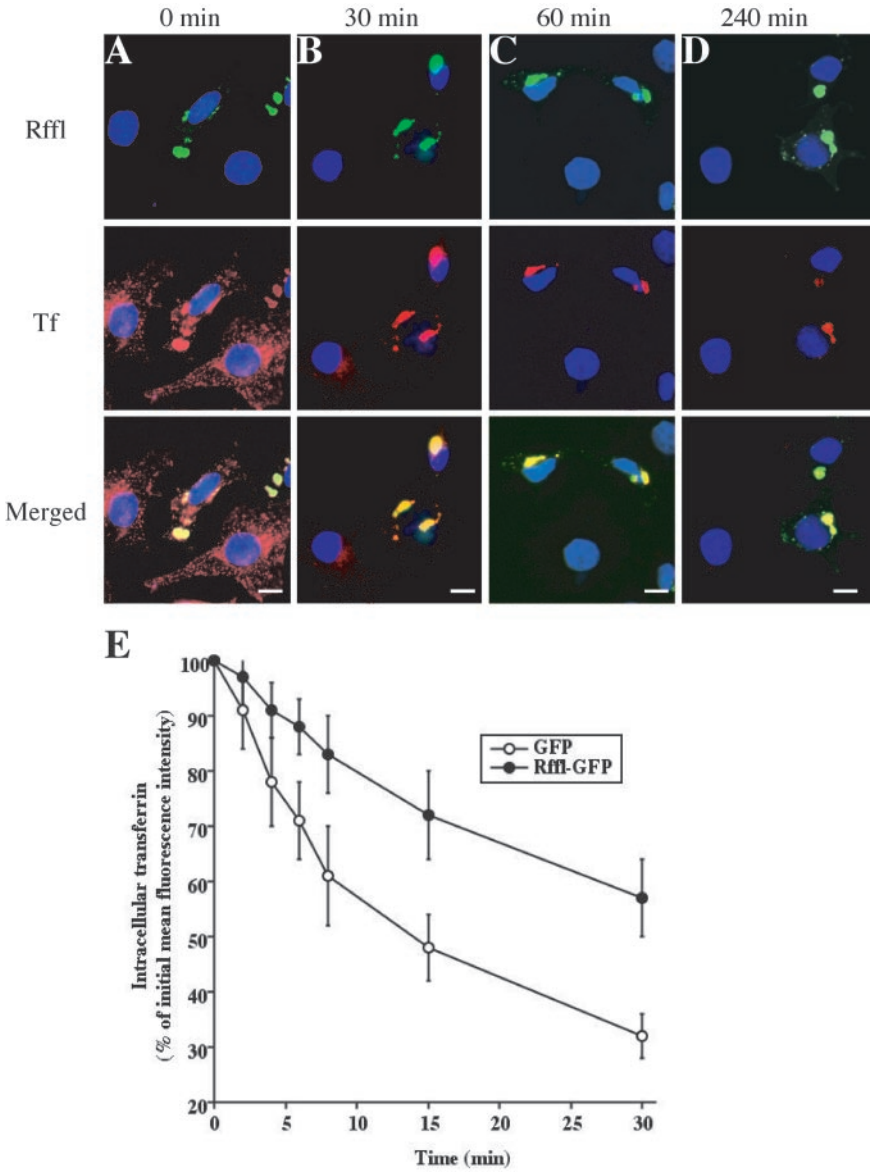

Figure 4. Effects of Rififylin-GFP on Tf recycling. (A–D): HeLa cells were transfected with Rffl-GFP–expressing vector. Sixteen hours later, the cells were washed and incubated for 30 min in medium without serum at 37°C. The cells were then allowed to internalize Alexa^{594}-Tf for 90 min at 37°C. The cells were either fixed at this point (0 min; A) or incubated for 30 min (B), 60 min (C), and 240 min (D) at 37°C. The cells were then fixed, stained with DAPI, and observed under a fluorescence microscope. Bars, 10 μm. (E) HeLa cells were transfected with expression vectors coding for Rffl-GFP or GFP as control. Sixteen hours later, the cells were washed, incubated for 30 min in medium without serum at 37°C, and incubated with Alexa^{633}-Tf for 60 min at 37°C. The remaining surface-bound Alexa^{633}-Tf was then removed by acid wash at 4°C. The cells were either kept on ice (0 min) or incubated for various times at 37°C. The intracellular associated fluorescence due to Alexa^{633}-Tf retained after each chase time was then quantified by flow cytometry, gating for transfected (GFP-positive) cells. The graph shows the average ± SD of three independent experiments.

Rffl-GFP were depleted of PtdIns(3)P by treatment with LY294002, an inhibitor of PtdIns(3)-kinases. In treated cells, we observed a much less intense vesicular EEA1 immunostaining, indicating that most EEA1 had been displaced by the treatment (Figure 7, A and B). In contrast, Rffl distribution was not modified by the treatment (Figure 7, A and B). Likewise, we observed that DFL-GFP distribution was not affected upon inhibitor treatment (Figure 7, C and D). Similar observations were made using wortmannin, a structurally unrelated inhibitor of PtdIns(3)-kinase activity. Increasing the concentration and/or the duration of wortmannin treatment had no effect on Rffl cellular distribution (our unpublished results). We next compared the effect of PtdIns(3)-kinases inhibitors and Rffl-GFP expression on Tf recycling (Figure 7E). Consistent with previous studies (Martys *et al.*, 1996; van Dam *et al.*, 2002), an inhibitory effect of LY294002 treatment on Tf recycling was observed. The inhibitory effect of LY294002 on Tf recycling was comparable to that induced by Rffl overexpression. Interestingly, a cumulative effect was observed when cells overexpressing Rffl were treated with LY294002 (Figure 7E). These data suggest that Rffl and PtdIns(3)-kinase inhibitors affect different recycling pathways.

DISCUSSION

The term ERC refers to a set of endocytic membranes, essentially tubules, that usually concentrate in the perinuclear region of the cell and in which membrane components following the endocytic recycling pathway travel. Few proteins were shown to localize to the ERC (Prekeris *et al.*, 1998; Lin *et al.*, 2001; Lindsay *et al.*, 2002; Lindsay and McCaffrey, 2002; Meyers and Prekeris, 2002; Wallace *et al.*, 2002a, 2002b). However, how these different proteins intervene in ERC function is largely unknown (Maxfield and McGraw, 2004).

In the present study, we have identified a novel protein, Rffl, that, when overexpressed in HeLa cells, localized to and induced the condensation of endosomal structures displaying TfR, Rab5, and Rab11 markers into several perinuclear globular structures. In contrast, the localization of EEA1, another marker of the early endocytic endosomes was not altered by Rffl overexpression. Finally, lysosomal markers,

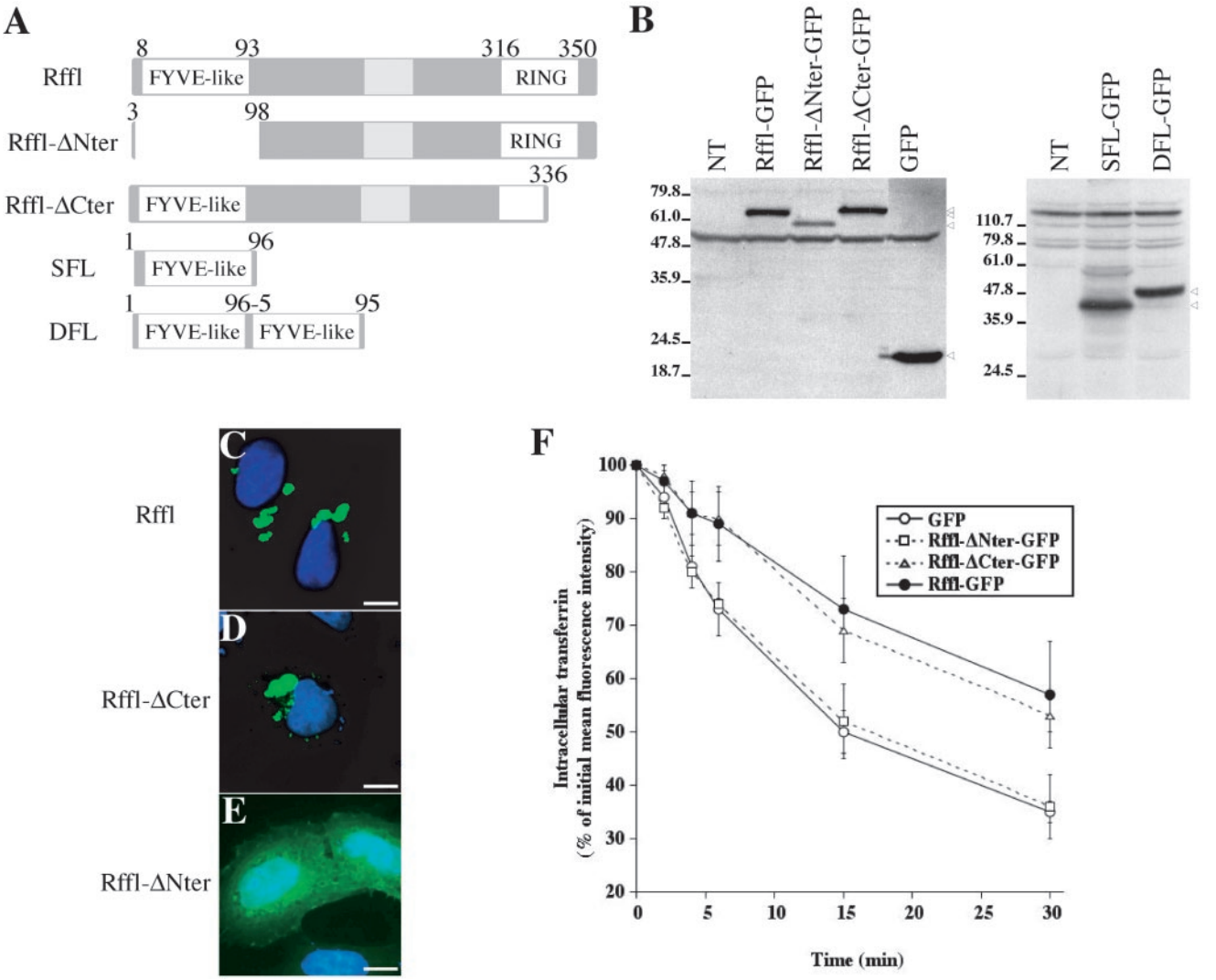

Figure 5. Analysis of deletion mutants lacking either the FYVE-like domain or the RING finger. (A) Schematic representation of Rffl deletions constructs. (B) Western blot detection of the various Rffl fusion proteins. Total cell lysates were prepared from either nontransfected (NT) or transfected HeLa cells. Full length Rffl-GFP (68 kDa), Rffl-ΔNter-GFP (58 kDa), Rffl-ΔCter-GFP (65 kDa), and GFP (27 kDa) were visualized with anti-GFP antibody (B, left panel). SFL-GFP (40 kDa) and DFL-GFP (49 kDa) were visualized with anti-Rffl antibodies raised against the FYVE-like domain (B, right panel). The arrowheads indicate the bands corresponding to the various fusion proteins. Nonspecific bands cross-reacting with both antibodies are also observed. (C–E) HeLa cells were transfected with Rffl-GFP (C), or Rffl-GFP deleted for either the carboxy-terminal domain (Rffl-ΔCter) (D), or the amino-terminal domain (Rffl-ΔNter) (E). Cells were fixed, stained with DAPI, and observed under a fluorescence microscope. Bars, 5 μm. (F) Quantification of the effect of the different constructs on Tf recycling was carried out by flow cytometry as in Figure 4. The graph shows the average ± SD of three independent experiments.

like Lamp2, or markers of secretory organelles, including the TGN, were not affected by Rffl overexpression. Consistently with confocal microscopy data, ultrastructural analysis showed that Rffl was mainly located on densely packed tubulovesicular membrane profiles. Altogether, these data suggest that the compartment affected by Rffl overexpression is the ERC.

Furthermore, recycling of TfR was inhibited by Rffl overexpression. Indeed, the aggregated recycling endosomes were accessible to endocytosed TfR-Tf complexes. However, recycling from the Rffl-positive compartment was delayed, Tf being still detected in the perinuclear region of transfected cells after several hours of chase. Recycling of membrane proteins can occur through at least two different routes that appear to depend on different molecular machineries (Hao and Maxfield, 2000; Sheff *et al.*, 2002). Rffl is involved in the recycling of only part of endocytosed TfR, suggesting that it affects the dynamics of a subdomain of recycling endosomes. The cumulative inhibitory effects of Rffl overexpression and of LY294002 treatment on Tf recycling suggests that Rffl acts mainly on a PtdIns(3)-kinase independent recycling pathway. This is consistent with our observations that Rffl affects the ERC and the proposal that, in HeLa cells, PtdIns(3)-kinase activity is required for recycling directly from early endosomes, a recycling route that bypasses the ERC (van Dam *et al.*, 2002).

We observed a major redistribution of Rab5 immunostaining upon Rffl overexpression. In normal cells, Rab5 overlaps extensively with EEA1 (Simonsen *et al.*, 1998; Lawe *et al.*, 2000), whereas it shows little colocalization with Rab11 (Sonnichsen *et al.*, 2000). In transfected cells, both Rab5 and Rab11 but not EEA1 concentrate in the aggregated recycling

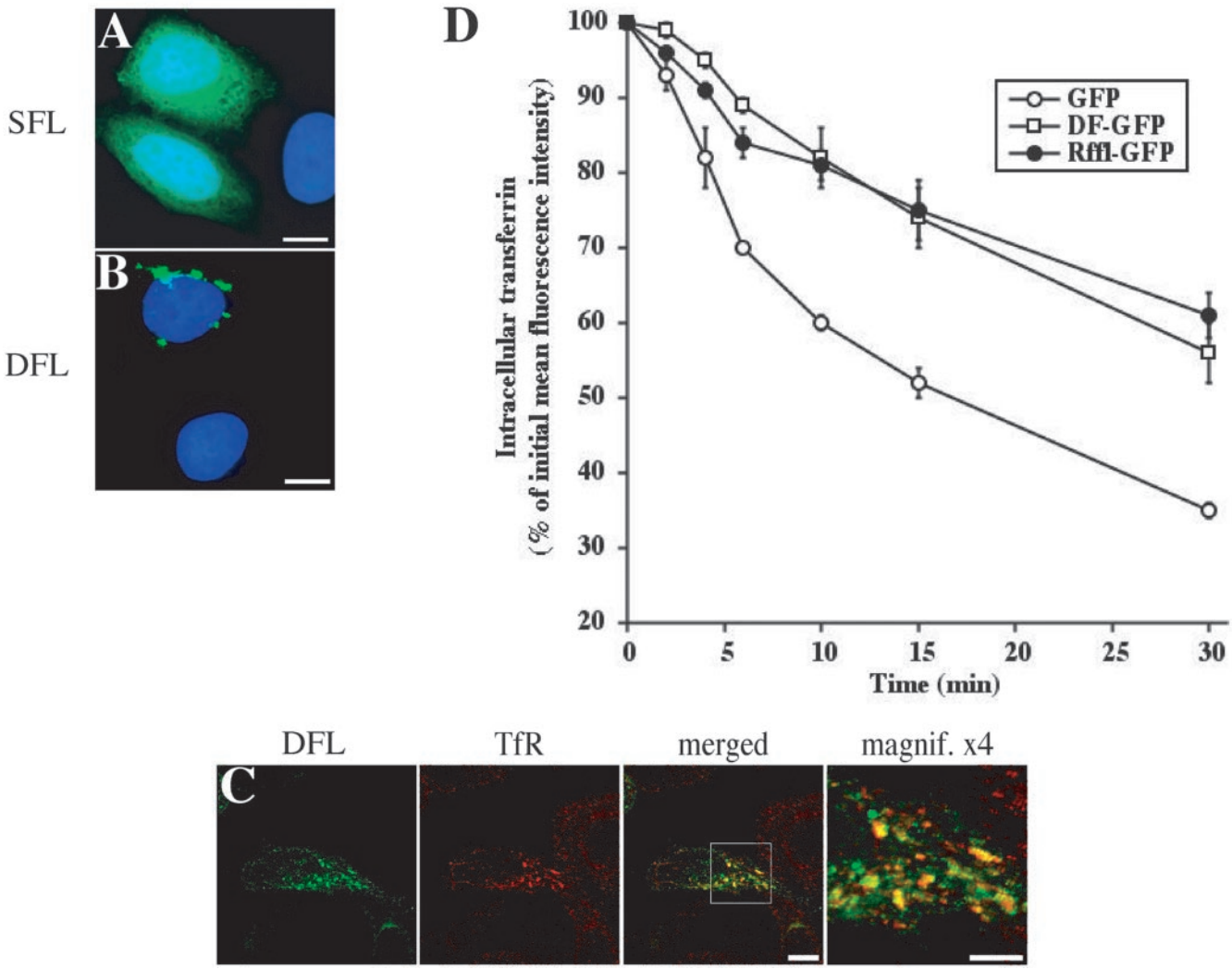

Figure 6. Analysis of the FYVE-like domain of Rififylin. (A and B) HeLa cells were transfected with SFL-GFP (A) or DFL-GFP (B) constructs, fixed, stained with DAPI, and observed under a fluorescence microscope. Sixteen hours after transfection, cells were fixed and processed for immunostaining with anti-TfR antibody and analyzed by confocal microscopy (C). Images show a medial orientation of a three-dimensional reconstruction. Bars, 10 μm. The right panel shows a higher magnification of the area delimited by the square inset showing the Rffl-positive compartment. Bars, 5 μm. (D) Quantification of the effect of the different constructs on Tf recycling was carried out by flow cytometry as in Figure 4. The graph shows the average ± SD of three independent experiments.

endosomes. This is a striking observation because EEA1 is a Rab5 effector (Simonsen *et al.*, 1998) and perturbations of the endocytic pathway that affect Rab5 without affecting EEA1 have not been reported so far. The way in which Rab5-positive endocytic membranes are disturbed by Rffl overexpression is unknown. However, it is unlikely to rely on direct physical interactions between Rab5 and Rffl, because the two proteins failed to interact in a yeast two-hybrid assay (F.Coumailleau and M.Cohen-Tannoudji, unpublished observations).

Concerning late endosomes, we noticed that some CD63-positive vesicles showed a tendency to be distributed around the aggregated Rffl-GFP–positive recycling endosomes. These surrounding endosomes appeared at the electron microscopy level as vacuoles with a limited amount of internal CD63-containing membranes and may correspond to early multivesicular bodies (MVB). We observed some Rffl staining on the limiting membrane of MVB-like endosomes, suggesting that Rffl overexpression might also perturb this compartment but to a much lesser extent than ERC.

Rffl is a previously uncharacterized protein that contains a zinc finger domain at both ends. The amino-terminal domain is similar to the well-characterized PtdIns(3)P-binding FYVE finger but presents noticeable departures from the consensus sequence in particular at the level of the core R(R/K)HHCR sequence, which is the principal site of interaction with PtdIns(3)P (Dumas *et al.*, 2001; Stenmark *et al.*, 2002). For this reason, we named it FYVE-like domain. Besides sequence similarities, the FYVE-like domain of Rffl shares other similarities with bona fide FYVE domains. Indeed, we have shown that it was necessary for the recruitment of Rffl to endocytic membranes. In addition, it is sufficient, if duplicated, to target GFP to endosomes. This is reminiscent of what has been described for the FYVE domains of EEA1 and Hrs (Stenmark *et al.*, 1996; Gillooly *et al.*, 2000; Lawe *et al.*, 2000). In these cases, the fact that isolated

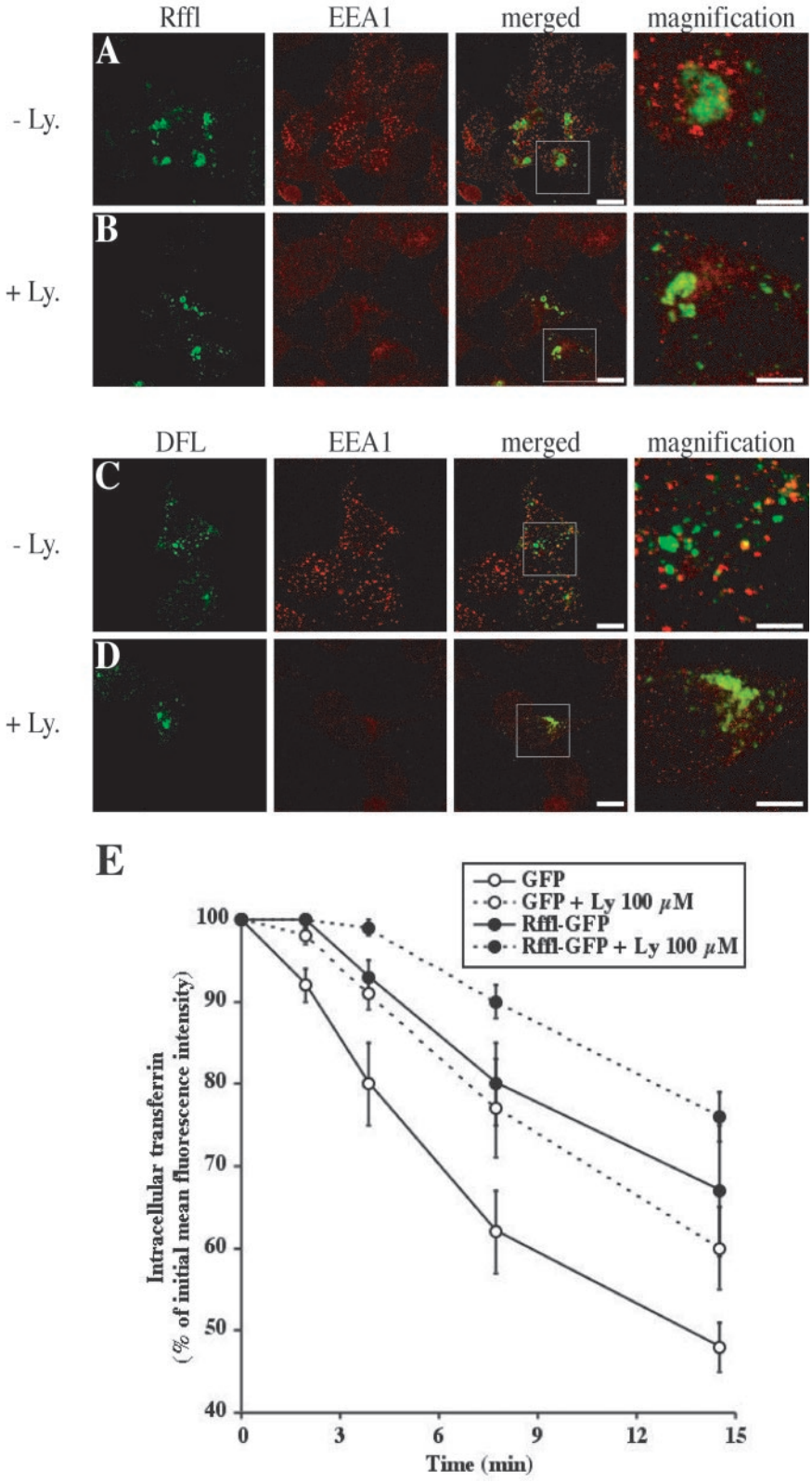

Figure 7. Effect of Rififylin-GFP is not dependent on PtdIns(3)-kinase activity. Sixteen hours after transfection with Rffl-GFP (A and B) or DFL-GFP (C and D), HeLa cells were incubated in medium alone (A and C) or containing 100 μM LY294002 (B and D) for 40 min at 37°C. The cells were then fixed and stained with an anti-EEA1 antibody and analyzed by confocal microscopy. Images show a medial orientation of a three-dimensional reconstruction. Bars, 10 μm. In each case, the right panel shows a higher magnification of the area delimited by the square inset showing the Rffl-positive compartment. Bars, 5 μm. (E) Recycling of Tf in Rffl-GFP and GFP-expressing cells in the absence or in the presence of 100 μM LY294002 was measured by flow cytometry as in Figure 4. The graph shows the average ± SD of three independent experiments. Ly: LY294002.

FYVE domains were not targeted to endosomes has been interpreted as due to a weak affinity for PtdIns(3)P that could be compensated by duplication. Similarly, the FYVE-like domain of Rffl may mediate weak interactions with components of recycling endocytic membranes, the nature and the identity of which remain to be identified. Importantly, major differences exist that distinguish the Rffl FYVE-like domain from bona fide FYVE domain. First, Rffl was

found on membranes with characteristic of recycling endosomes and did not overlap with EEA1-positive early endosomes membranes. On the contrary, bona fide FYVE domain-containing proteins localize to PtdIns(3)P-containing membranes, i.e., early endosomes and internal vesicles of the MVB (Gillooly *et al.*, 2000). These proteins play important roles in endocytic membrane trafficking such as early endosome fusion (EEA1; Simonsen *et al.*, 1998), traffic from early endosome to recycling endosomes (Rabip4 and Rabenosyn-5; Nielsen *et al.*, 2000; Cormont *et al.*, 2001; de Renzis *et al.*, 2002), or from early endosome to late endosomes (Hrs and PikFYVE; Komada and Soriano, 1999; Ikonomov *et al.*, 2001; Raiborg *et al.*, 2002) but are not involved in traffic from ERC to plasma membrane. A second important difference is that endosomal localization of full-length Rffl or DFL-GFP is independent of PtdIns(3)-kinase activity, whereas that of bona fide FYVE domain-containing proteins is not. This indicates that, as already suggested by the amino-acid sequence, Rffl FYVE-like domain does not bind to PtdIns(3)P. It is therefore not surprising that Rffl does not localize to PtdIns(3)P-enriched membranes. Of special interest will be the characterization of the natural ligand of the FYVE-like domain.

The second zinc finger domain of Rffl is a carboxy-terminal RING finger motif. Within the past few years, evidence has accumulated arguing in favor of a general role in ubiquitination for RING finger-containing proteins (Freemont, 2000; Weissman, 2001). Recently, it has been shown that SAKURA, the rat ortholog of Rffl, exhibited E3 ubiquitin ligase activity in vitro and ex vivo (Araki *et al.*, 2003). However, the RING domain of Rffl does not appear to participate in the recycling inhibition mediated by Rffl overexpression because similar perturbations of recycling endosomes were obtained upon transfection of full-length and RING finger-deleted version of Rffl (Rffl-ΔCter).

Exactly how Rffl could affect the morphology and the function of the ERC is unclear. However, it should be noted that inhibition of Tf recycling was obtained by overexpressing the full-length protein. This is in contrast with other proposed ERC regulatory proteins for which recycling was affected upon overexpression of constitutively active or inactive forms (Rab4, Rab11) or dominant negative mutated or truncated proteins (RCP, Rme1, Rab11BP/Rabphillin11), whereas the overexpression of full-length proteins had little or no effect on the Tf recycling pathway (van der Sluijs *et al.*, 1992; Ullrich *et al.*, 1996; Zeng *et al.*, 1999; Wilcke *et al.*, 2000; Lin *et al.*, 2001; McCaffrey *et al.*, 2001; Lindsay *et al.*, 2002). Therefore, the phenotype observed in cells overexpressing Rffl may be due to enhancement of the normal functions of Rffl, resulting in excess Rffl activity. Underlying this hypothesis is the assumption that in untransfected cells Rffl is a limiting component. When the FYVE-like domain of Rffl was removed, the protein remained cytosolic and inhibition of Tf recycling was no longer observed. This suggests that association of Rffl with ERC membranes is necessary for its interference with recycling. Interestingly, we found that DFL-GFP has an inhibitory effect on recycling. This could be the consequence of the occupancy of FYVE-like domain binding sites on ERC membranes by DFL-GFP and the consecutive displacement of endogenous Rffl or other proteins targeted to ERC membranes through similar mechanism.

In conclusion, we have characterized a new protein that, when overexpressed, alters both the morphology and the function of the ERC. Further studies on how Rffl overexpression inhibits recycling from ERC to the plasma membrane will certainly help to understand the molecular mechanisms underlying membranes proteins trafficking along this poorly characterized compartment.

ACKNOWLEDGMENTS

We thank Karim Nacerddine for helping in the production of recombinant fusion protein; Serge Benichou for continuous support and helpful suggestions; Katy Janvier, Corinne Leprince, and Sonia Martinez for technical advice; Jean Salamero and Bruno Goud for anti-Rab11 and anti-Rab6 antibodies; and the IMAGE consortium for the EST clone 567814. The sequences reported in this paper have been submitted to the GenBank™/EBI Data Bank with accession numbers AY163902 and AY163903. We are also very grateful to Pascal Roux and Emmanuelle Perret, Plateforme d'Imagerie Dynamique, Institut Pasteur, and Marie-Christine Wagner, Plateforme de Cytométrie, Institut Pasteur, for technical assistance. This work was supported by the Centre National de la Recherche Scientifique, the Institut Pasteur and the "Action concertée incitative Biologie Cellulaire, Moléculaire et Structurale" from the Ministère de l'Education Nationale, de la Recherche et de la Technologie. F.C., V.D., and S.L.B. received funding from the Ministère de l'Education Nationale, de la Recherche et de la Technologie. F.C. and S.L.B. were recipients of a fellowship from the Association pour la Recherche sur le Cancer.

REFERENCES

Apodaca, G., Katz, L.A., and Mostov, K.E. (1994). Receptor-mediated transcytosis of IgA in MDCK cells is via apical recycling endosomes. J. Cell Biol. *125*, 67–86.

Araki, K. *et al.* (2003). A palmitoylated RING finger ubiquitin ligase and its homologue in the brain membranes. J. Neurochem. *86*, 749–762.

Babinet, C., Richoux, V., Guenet, J.L., and Renard, J.P. (1990). The DDK inbred strain as a model for the study of interactions between parental genomes and egg cytoplasm in mouse preimplantation development. Development Suppl. 81–87.

Bucci, C., Parton, R.G., Mather, I.H., Stunnenberg, H., Simons, K., Hoflack, B., and Zerial, M. (1992). The small GTPase rab5 functions as a regulatory factor in the early endocytic pathway. Cell *70*, 715–728.

Burd, C.G., and Emr, S.D. (1998). Phosphatidylinositol(3)-phosphate signaling mediated by specific binding to RING FYVE domains. Mol. Cell *2*, 157–162.

Cohen-Tannoudji, M., Baldacci, P.A., Kress, C., Richoux-Duranthon, V., Renard, J.P., and Babinet, C. (1996). Genetic and molecular studies on *Om*, a locus controlling mouse preimplantation development. Acta. Genet. Med. Gemellol. *45*, 3–14.

Cohen-Tannoudji, M., Vandormael-Pournin, S., Le Bras, S., Coumailleau, F., Babinet, C., and Baldacci, P. (2000). A 2-Mb YAC/BAC-based physical map of the ovum mutant (Om) locus region on mouse chromosome 11. Genomics *68*, 273–282.

Cormont, M., Mari, M., Galmiche, A., Hofman, P., and Le Marchand-Brustel, Y. (2001). A FYVE-finger-containing protein, Rabip4, is a Rab4 effector involved in early endosomal traffic. Proc. Natl. Acad. Sci. USA *98*, 1637–1642.

de Renzis, S., Sonnichsen, B., and Zerial, M. (2002). Divalent Rab effectors regulate the sub-compartmental organization and sorting of early endosomes. Nat. Cell Biol. *4*, 124–133.

Dumas, J.J., Merithew, E., Sudharshan, E., Rajamani, D., Hayes, S., Lawe, D., Corvera, S., and Lambright, D.G. (2001). Multivalent endosome targeting by homodimeric EEA1. Mol. Cell *8*, 947–958.

Duprez, V., Cornet, V., and Dautry-Varsat, A. (1988). Down-regulation of high affinity interleukin 2 receptors in a human tumor T cell line. Interleukin 2 increases the rate of surface receptor decay. J. Biol. Chem. *263*, 12860–12865.

Freemont, P.S. (2000). RING for destruction? Curr. Biol. *10*, R84–R87.

Gaullier, J.M., Simonsen, A., D'Arrigo, A., Bremnes, B., Stenmark, H., and Aasland, R. (1998). FYVE fingers bind PtdIns(3)P. Nature *394*, 432–433.

Ghosh, R.N., Mallet, W.G., Soe, T.T., McGraw, T.E., and Maxfield, F.R. (1998). An endocytosed TGN38 chimeric protein is delivered to the TGN after trafficking through the endocytic recycling compartment in CHO cells. J. Cell Biol. *142*, 923–936.

Gillooly, D.J., Morrow, I.C., Lindsay, M., Gould, R., Bryant, N.J., Gaullier, J.M., Parton, R.G., and Stenmark, H. (2000). Localization of phosphatidylinositol 3-phosphate in yeast and mammalian cells. EMBO J. *19*, 4577–4588.

Gorvel, J.P., Chavrier, P., Zerial, M., and Gruenberg, J. (1991). Rab5 controls early endosome fusion in vitro. Cell *64*, 915–925.

Hao, M., and Maxfield, F.R. (2000). Characterization of rapid membrane internalization and recycling. J. Biol. Chem. *275*, 15279–15286.

Ikonomov, O.C., Sbrissa, D., and Shisheva, A. (2001). Mammalian cell morphology and endocytic membrane homeostasis require enzymatically active phosphoinositide 5-kinase PIKfyve. J. Biol. Chem. *276*, 26141–26147.

Knight, A., Hughson, E., Hopkins, C.R., and Cutler, D.F. (1995). Membrane protein trafficking through the common apical endosome compartment of polarized Caco-2 cells. Mol. Biol. Cell *6*, 597–610.

Komada, M., and Soriano, P. (1999). Hrs, a FYVE finger protein localized to early endosomes, is implicated in vesicular traffic and required for ventral folding morphogenesis. Genes Dev. *13*, 1475–1485.

Lapierre, L.A. *et al.* (2001). Myosin vb is associated with plasma membrane recycling systems. Mol. Biol. Cell *12*, 1843–1857.

Lawe, D.C., Patki, V., Heller-Harrison, R., Lambright, D., and Corvera, S. (2000). The FYVE domain of early endosome antigen 1 is required for both phosphatidylinositol 3-phosphate and Rab5 binding. Critical role of this dual interaction for endosomal localization. J. Biol. Chem. *275*, 3699–3705.

Le Bras, S., Cohen-Tannoudji, M., Guyot, V., Vandormael-Pournin, S., Coumailleau, F., Babinet, C., and Baldacci, P. (2002). Transcript map of the *Ovum mutant* (*Om*) locus: isolation by exon trapping of new candidates genes for the DDK syndrome. Gene *296*, 75–86.

Lin, S.X., Grant, B., Hirsh, D., and Maxfield, F.R. (2001). Rme-1 regulates the distribution and function of the endocytic recycling compartment in mammalian cells. Nat. Cell Biol. *3*, 567–572.

Lindsay, A.J., Hendrick, A.G., Cantalupo, G., Senic-Matuglia, F., Goud, B., Bucci, C., and McCaffrey, M.W. (2002). Rab coupling protein (RCP), a novel Rab4 and Rab11 effector protein. J. Biol. Chem. *277*, 12190–12199.

Lindsay, A.J., and McCaffrey, M.W. (2002). Rab11-FIP2 functions in transferrin recycling and associates with endosomal membranes via Its COOH-terminal domain. J. Biol. Chem. *277*, 27193–27199.

Liou, W., Geuze, H.J., and Slot, J.W. (1996). Improving structural integrity of cryosections for immunogold labeling. Histochem. Cell Biol. *106*, 41–58.

Martys, J.L., Wjasow, C., Gangi, D.M., Kielian, M.C., McGraw, T.E., and Backer, J.M. (1996). Wortmannin-sensitive trafficking pathways in Chinese hamster ovary cells. Differential effects on endocytosis and lysosomal sorting. J. Biol. Chem. *271*, 10953–10962.

Maxfield, F.R., and McGraw, T.E. (2004). Endocytic recycling. Nat. Rev. Mol. Cell Biol. *5*, 121–132.

McCaffrey, M.W., Bielli, A., Cantalupo, G., Mora, S., Roberti, V., Santillo, M., Drummond, F., and Bucci, C. (2001). Rab4 affects both recycling and degradative endosomal trafficking. FEBS Lett. *495*, 21–30.

Mellman, I. (1996). Endocytosis and molecular sorting. Annu. Rev. Cell Dev. Biol. *12*, 575–625.

Meyers, J.M., and Prekeris, R. (2002). Formation of mutually exclusive Rab11 complexes with members of the family of Rab11-interacting proteins regulates Rab11 endocytic targeting and function. J. Biol. Chem. *277*, 49003–49010.

Mukherjee, S., Ghosh, R.N., and Maxfield, F.R. (1997). Endocytosis. Physiol. Rev. *77*, 759–803.

Nielsen, E., Christoforidis, S., Uttenweiler-Joseph, S., Miaczynska, M., Dewitte, F., Wilm, M., Hoflack, B., and Zerial, M. (2000). Rabenosyn-5, a novel Rab5 effector, is complexed with hVPS45 and recruited to endosomes through a FYVE finger domain. J. Cell Biol. *151*, 601–612.

Patki, V., Lawe, D.C., Corvera, S., Virbasius, J.V., and Chawla, A. (1998). A functional PtdIns(3)P-binding motif. Nature *394*, 433–434.

Prekeris, R., Klumperman, J., Chen, Y.A., and Scheller, R.H. (1998). Syntaxin 13 mediates cycling of plasma membrane proteins via tubulovesicular recycling endosomes. J. Cell Biol. *143*, 957–971.

Raiborg, C., Bache, K.G., Gillooly, D.J., Madshus, I.H., Stang, E., and Stenmark, H. (2002). Hrs sorts ubiquitinated proteins into clathrin-coated microdomains of early endosomes. Nat. Cell Biol. *4*, 394–398.

Raposo, G., Kleijmeer, M.J., Posthuma, G., Slot, J.W., and Geuze, H.J. (1997). Immunogold labeling of ultrathin cryosections: application in immunology. In: Handbook of Experimental Immunology, vol. 4, 5th ed., ed. I.L.A. Herzenberg, D. Weir, and L.A. Herzenberg, C. Blackwell, Cambridge, MA: Blackwell Science, Chapter 208, 1–11.

Saurin, A.J., Borden, K.L., Boddy, M.N., and Freemont, P.S. (1996). Does this have a familiar RING? Trends Biochem. Sci. *21*, 208–214.

Sheff, D., Pelletier, L., O'Connell, C.B., Warren, G., and Mellman, I. (2002). Transferrin receptor recycling in the absence of perinuclear recycling endosomes. J. Cell Biol. *156*, 797–804.

Simonsen, A. *et al.* (1998). EEA1 links PI(3)K function to Rab5 regulation of endosome fusion. Nature *394*, 494–498.

Slot, J.W., Geuze, H.J., Gigengack, S., Lienhard, G.E., and James, D. (1991). Immuno-localization of the insulin regulatable glucose transporter in brown adipose tissue of the rat. J. Cell Biol. *113*, 123–135.

Sonnichsen, B., De Renzis, S., Nielsen, E., Rietdorf, J., and Zerial, M. (2000). Distinct membrane domains on endosomes in the recycling pathway visualized by multicolor imaging of Rab4, Rab5, and Rab11. J. Cell Biol. *149*, 901–914.

Stenmark, H., Aasland, R., and Driscoll, P.C. (2002). The phosphatidylinositol 3-phosphate-binding FYVE finger. FEBS Lett. *513*, 77–84.

Stenmark, H., Aasland, R., Toh, B.H., and D'Arrigo, A. (1996). Endosomal localization of the autoantigen EEA1 is mediated by a zinc-binding FYVE finger. J. Biol. Chem. *271*, 24048–24054.

Stenmark, H., Valencia, A., Martinez, O., Ullrich, O., Goud, B., and Zerial, M. (1994). Distinct structural elements of rab5 define its functional specificity. EMBO J. *13*, 575–583.

Stumptner-Cuvelette, P., Jouve, M., Helft, J., Dugast, M., Glouzman, A.S., Jooss, K., Raposo, G., and Benaroch, P. (2003). Human immunodeficiency virus-1 Nef expression induces intracellular accumulation of multivesicular bodies and major histocompatibility complex class II complexes: potential role of phosphatidylinositol 3-kinase. Mol. Biol. Cell *14*, 4857–4870.

Ullrich, O., Reinsch, S., Urbe, S., Zerial, M., and Parton, R.G. (1996). Rab11 regulates recycling through the pericentriolar recycling endosome. J. Cell Biol. *135*, 913–924.

van Dam, E.M., Ten Broeke, T., Jansen, K., Spijkers, P., and Stoorvogel, W. (2002). Endocytosed transferrin receptors recycle via distinct dynamin and phosphatidylinositol 3-kinase-dependent pathways. J. Biol. Chem. *277*, 48876–48883.

van der Sluijs, P., Hull, M., Webster, P., Male, P., Goud, B., and Mellman, I. (1992). The small GTP-binding protein rab4 controls an early sorting event on the endocytic pathway. Cell *70*, 729–740.

Wallace, D.M., Lindsay, A.J., Hendrick, A.G., and McCaffrey, M.W. (2002a). The novel Rab11-FIP/Rip/RCP family of proteins displays extensive homo- and hetero-interacting abilities. Biochem. Biophys. Res. Commun. *292*, 909–915.

Wallace, D.M., Lindsay, A.J., Hendrick, A.G., and McCaffrey, M.W. (2002b). Rab11-FIP4 interacts with Rab11 in a GTP-dependent manner and its overexpression condenses the Rab11 positive compartment in HeLa cells. Biochem. Biophys. Res. Commun. *299*, 770–779.

Weissman, A.M. (2001). Themes and variations on ubiquitylation. Nat. Rev. Mol. Cell. Biol. *2*, 169–178.

Wilcke, M., Johannes, L., Galli, T., Mayau, V., Goud, B., and Salamero, J. (2000). Rab11 regulates the compartmentalization of early endosomes required for efficient transport from early endosomes to the trans-golgi network. J. Cell Biol. *151*, 1207–1220.

Zeng, J. *et al.* (1999). Identification of a putative effector protein for rab11 that participates in transferrin recycling. Proc. Natl. Acad. Sci. USA *96*, 2840–2845.

Zerial, M., and McBride, H. (2001). Rab proteins as membrane organizers. Nat. Rev. Mol. Cell. Biol. *2*, 107–117.